Available online at www.sciencedirect.com

ScienceDirect

Physics Procedia 56 (2014) 1171 – 1181

Physics Procedia

8th International Conference on Photonic Technologies LANE 2014

Laser Surface Pre-treatment of Aluminium for Hybrid Joints with Glass Fibre Reinforced Thermoplastics

André Heckert[a,]*, Michael F. Zaeh[a]

[a]*Institute for Machine Tools and Industrial Management (iwb), Technische Universität München, Boltzmannstrasse 15, 85748 Garching, Germany*

Abstract

Lightweight construction is a major trend in the automotive industry. The connection of fibre reinforced plastics with aluminium is consequently seen as promising prospect. In this regard, thermal joining can be applied for bonding of such hybrid joints. But in order to create a load bearing metal plastic joint, the surface of the metal has to be pre-treated. Recent research has shown that with laser surface pre-treatment high joint strengths are obtained. Yet there are a variety of laser sources and manufacturable surface topographies with structure sizes ranging from macroscopic to nanoscopic profiles. Within this work, macroscopic, microscopic and nanoscopic laser processed structures are created on aluminium and consequently joined to glass fibre reinforced thermoplastics of different fibre length and fibre content. High shear tensile strengths of up to 42 N/mm² were obtained depending on the allocated material and the surface pre-treatment.

Peer-review under responsibility of the Bayerisches Laserzentrum GmbH

Keywords: Thermal joining; thermoplastic metal hybrids; laser surface pre-treatment; macroscopic structure; microscopic structure; nanoscopic structure.

1. Motivation

The amount of lightweight parts in automobiles will increase from nowadays 30% up to 70% by 2030 as shown in a recent study (McKinsey & Company 2012). One reason for this change is the legal regulation by the German government that is going to state an upper limit for the average CO2-emission of 95 g/km for the fleet of a vehicle

* Corresponding author. Tel.: +49-(0)89-289-15589 ; fax: +49-(0)89-289-15555 .
E-mail address: Andre.Heckert@iwb.tum.de

Peer-review under responsibility of the Bayerisches Laserzentrum GmbH
doi:10.1016/j.phpro.2014.08.032

manufacturer. Especially for the German car industry, which accounts for the biggest share of the premium car segment, the emission reduction can only be achieved by both employing lightweight materials and electric drives. Thus, depending on the car classification, different lightweight material mixes will become profitable. In this context, the bonding of aluminium, which is already used as lightweight material in automobiles, with fibre reinforced plastics (FRP) is seen as a promising prospect (McKinsey & Company 2012).

Furthermore, it has recently become possible to manufacture thermoplastics (TP) with endless fibre reinforcements in high quantities (BASF 2013). Those materials obtain properties superior to those of short fibre reinforced thermoplastics and to aluminium. Even though the endless fibre reinforced TPs do not attain the mechanical strength and stiffness of reinforced thermosets, they are beneficial in manufacturing because of the fusibility.

This characteristic enables thermal joining. Thermal joining is distinguished by short processing times, no additional weight and no fibre damage in comparison to the state of the art of joining technologies like bolted connections and adhesive bonding (Ageorges and Ye 2002).

But in order to produce a load bearing joint of fibre reinforced TPs and metals with thermal joining, it is necessary to apply a surface pre-treatment to the metal joining partner prior to bonding. This can be done by mechanical, chemical, electrochemical or physical processes (Habenicht 2009). Recent research has shown that laser surface treatment allows a flexible manufacturing of the metal surface with bonding strength equal to electrochemical surface pre-treatments (Rechner 2012, Kurtovic et al. 2013). There are numerous processing strategies which result in diverse surface structures on the metal. This paper investigates the potential of three different laser processed surface structures in the macroscopic, microscopic and nanoscopic scale which can be used for thermal joining of fibre reinforced TPs with aluminium. Furthermore, it is shown that the fibre length and the fibre volume content of the FRP significantly influence the mechanical strength of the hybrid material joint.

2. State of the art

2.1. Thermal joining of metal plastic hybrid joints by laser radiation

Melting the TP is necessary to produce a metal plastic hybrid joint by thermal joining. There are various applicable ways for heat generation such as induction, ultrasonics, heating elements or laser radiation (Ageorges and Ye 2002). In this regard, laser beam joining is beneficial because it enables a controllable energy input, fast processing times, flexible joint configurations, a double-sided accessibility and an independent definition of pressure and heat generation.

There are two procedural principles of the laser beam joining for hybrid joints:

- Transmission joining (TJ)
- Heat-conduction joining (HCJ)

For TJ the laser beam is transmitted through the plastic material and heats the metal joining partner, see Fig. 1a. Consequently the temperature of the metal plastic interface rises until the plastic is molten. The joint is established as soon as the plastic wets the metal and re-solidifies. This process can only be applied for plastics which show a high level of transparency for electromagnetic radiation of the laser wavelength. Glass fibres (GF) and especially carbon fibres reduce the transparency of the material (Abed and Knapp 2007). Consequently, this process is not applicable for highly fibre reinforced TPs. There are several publications dealing with TJ and HCJ for metal TP joints which are summarized in Table 1.

HCJ works independently of the fibre volume content since the metal surface is irradiated directly by the laser beam, see Fig. 1b. The heat is consequently conducted to the metal plastic interface which leads to the melting of the plastic partner in the boundary layer.

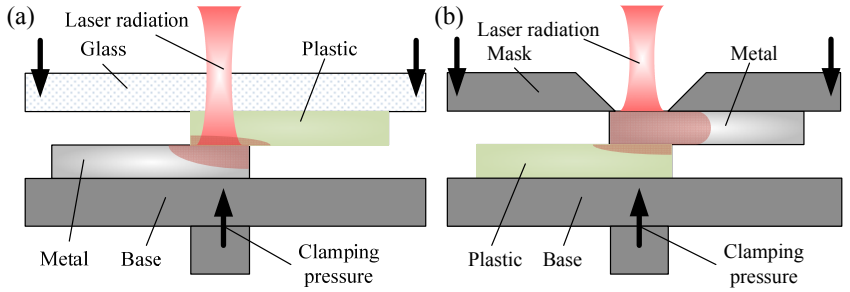

Fig. 1. (a) Laser transmission joining with a glass as clamping device and (b) heat conduction joining with a mask.

Since this laser beam joining process does not require high beam quality, diode lasers (DL) and Nd:YAG lasers are frequently used, see Table 1. In addition, plastics are transparent (Abed and Knapp 2007) and aluminium is well absorptive (Bartl and Baranek 2004) for laser radiation in the wave length range between 808 nm and 1070 nm.

Table 1. State of the art in laser joining of metal thermoplastic joints.

Author	Metal	Plastic	Process	Laser	Surface treatment
Amend et al. (2013)	Aluminium	PC*, PA 6**, PA 6 GF30**	HCJ, TJ	DL	Laser
Bergmann and Stambke (2012)	Steel	PA 66*, PA 6 GF45**	HCJ, TJ	DL	Stamping, sandblasting
Cenigaonaindia et al. (2012)	Stainless steel	PA 6	TJ	DL	Milling
Engelmann et al. (2013)	Stainless steel	PA 6 GF Laminate	HCJ	DL	Laser
Fortunato et al. (2010)	Stainless steel	PA 66*/**,PA 66 GF35/CF40**	HCJ, TJ	DL	-
Kawahito et al. (2006)	Stainless steel	PET*/**, PA*/**, PC*/**, PP*/**	HCJ, TJ	Nd:YAG, DL	-
Niwa et al. (2007)	Stainless steel	PET*/**, PA**, PA GF30**	HCJ, TJ	Nd:YAG, DL	-
Katayama and Kawahito (2008)	Stainless steel	PET	TJ	DL	-
Roesner et al. (2011)	Stainless steel	PC, PA 66, PA 66 GF30	HCJ	DL	Laser
Roesner et al. (2013)	-	PC	TJ	DL	Laser
Wahba et al. (2011)	Magnesium	PET	HCJ, TJ	DL	Laser, grinding

* Transmission joining (TJ); ** Heat conduction joining (HCJ)

In order to create defined joining conditions, the joining partners are clamped. Two methods have been identified: clamping by glass or clamping by a mask, see Fig. 1. In Cenigaonaindia et al. (2012) a rigid transparent quartz glass was placed on top of the clamping system and the force was applied through pneumatic actuators. Other authors, as Bergmann and Stambke (2012) as well as Roesner et al. (2011), reported on clamping of the specimens but did not specify the clamping device. In Flock (2012) it was shown that the clamping pressure has influence on the resulting joint properties. Hence, the clamping device has to be considered as an additional joining parameter.

2.2. Laser surface pre-treatment for the metal joining partner

Table 1 shows that several authors utilise a surface pre-treatment prior to bonding in order to enhance the properties of the metal plastic joints. All authors observed an increasing joint strength after modifying the surface of the metal joining partner.

The surface pre-treatment is well established for adhesive bonds and it aims at the production of a defined surface. According to Habenicht (2009) the methods of surface pre-treatment can be classified into the following:

- Mechanical pre-treatment (e.g. abrasive blasting)
- Combined surface pre-treatments (e.g. SiliCoater process, SACO method)
- Physical surface pre-treatments (e.g. atmospheric pressure plasma, corona discharge, laser treatment)

- Chemical surface pre-treatment (e.g. steeping in a corrosive fluid)
- Electrochemical surface pre-treatment (e.g. phosphoric acid anodisation - PAA)

The most extensive knowledge exists on electrochemical surface pre-treatment since it is applied for high performance adhesive bonds in the aircraft industry. Due to the costly procedure and the toxicity of the acids, the process is not applicable for instance in the line production of automobiles. Instead, for adhesive bonding, the surfaces are usually degreased and mechanically pre-treated by abrasive blasting. In principle, the surface pre-treatment has to be chosen depending on cost, required strength and aging characteristics. (Habenicht 2009)

Investigations of Kurtovic et al. (2013), Zimmermann et al. (2012) and Rechner (2012) on laser surface pre-treatment showed that adhesive bonds could be created, which had even superior mechanical properties when compared to electrochemical pre-treatments. In addition, the laser surface pre-treatment is environmentally friendly since no hazardous additives are used. Furthermore, modern pulsed laser systems offer both high power and repetition rate, which enable an economically feasible process (Beyer et al. 2013).

Currently there are numerous approaches for processing surfaces with laser radiation. The following table classifies the different laser surface pre-treatments. Four groups of laser processed features are proposed that differ in the structure height, see Table 2.

Table 2. Classification of groups for the laser surface pre-treatment.

Group	Description	Structure height	Identifiable by
I	No nano/micro/macro roughness	No surface modification	-
II	Macroscopic structures	> 200 µm	Eye
III	Microscopic structures	100 nm - 200 µm	Optical microscope
IV	Nanoscopic structures	< 100 nm	Scanning electron microscope

Venables (1984) classified different surfaces produced by chemical and electrochemical pre-treatments for adhesive bonding applications and consequently introduced microscopic and macroscopic structures. This classification was utilised by Mertens et al. (2012) who added the term nanoscopic. In order to account for the span in structure heights, which can be processed via laser, the range and the description of the groups was modified. In Table 3, recent research is summarized and classified into the presented four groups.

Table 3. State of the art in laser surface pre-treatment.

Group	Author	Laser	Pulse width	Substrate	Bonding application
I	Lu et al. (1994)	KrF-excimer	20 ns	Aluminium	-
I	Rotel et al. (2000)	ArF-excimer	pulsed	Aluminium	Adhesive bonding
I	Critchlow et al. (1997)	CO_2	pulsed	Aluminium	Adhesive bonding
I	Turner et al. (2006)	CO_2	cw	Titanium	-
I	Rechner et al. (2010)	Nd:YAG	ns	Aluminium	Adhesive bonding
II	Earl et al. (2012)	Yb:fibre	cw	Titanium	-
II	Blackburn and Hilton (2011)	Yb:fibre	cw	Titanium	-
III	Demir et al. (2010)	Yb:fibre	100 ns	Stainless steel	-
III	Holtkamp et al. (2010)	Nd:YAG	-	Stainless steel	HCJ
III	Roesner et al. (2011)	Nd:YAG	µs	Stainless steel	HCJ
III	Engelmann et al. (2013)	Yb:fibre	cw	Stainless steel	HCJ
III	Amend et al. (2013)	Nd:YAG	ns	Aluminium	HCJ, TJ
IV	Rechner (2012)	Nd:YAG, Yb:fibre	ns	Aluminium	Adhesive bonding
IV	Zimmermann et al. (2012)	Nd:YAG	80 ns	Titanium	Adhesive bonding
IV	Kurtovic et al. (2013)	Nd:YVO_4	ns	Titanium	Adhesive bonding

Group I refers to laser pre-treatments which are not intended to modify the surface of the metal substrate. The energy input via laser is only used for removing residues like oil or grease. Infrared (IR) and ultraviolet (UV) lasers as well as pulsed and continuous wave (cw) laser sources were utilised. Lu et al. (1994) proposed that the UV laser is the most feasible for cleaning of the surface since the photon energy of the laser radiation is close to the binding energy of organic residues. Rotel et al. (2000), Rechner et al. (2010) and Critchlow et al. (1997) used the pre-treatment for adhesive bonding to aluminium and observed an increase in joint strength.

Group II refers to structures with heights greater than 200 µm. Consequently, they can be identified without the aid of microscopy. In Blackburn and Hilton (2011) and Earl et al. (2012) the process Surfi-Sculpt is employed, which was first discovered and patented by The Welding Institute (TWI). Surfi-Sculpt utilises the humping effect which results from disruptions of the vapour capillary in keyhole welding. At high welding speeds with a focussed cw-laser beam a molten bath is created that moves against the laser trajectory. Through repetitions, features can be created with heights of several millimetres. The authors proposed a deployment of the generated features for joining applications, but did not investigate this subject in detail.

Microscopic structures with heights from 100 nm up to 200 µm are classified into Group III. Those structures can be identified by optical microscopy. In order to create microscopic structures, mostly IR pulsed laser systems were used, see Table 3. All authors produced either a line, grid or crater structure and hence undercuts on the metal surface. Amend et al. (2013), Holtkamp et al. (2010), Roesner et al. (2011) and Engelmann et al. (2013) already utilised the microscopic laser surface pre-treatment to improve the joint properties of the metal TP hybrids.

Structure sizes below 100 nm are detectable only by high resolution scanning electron microscopy (SEM) and are consequently classified into Group IV. Kurtovic et al. (2013), Rechner (2012) and Zimmermann et al. (2012) created those structures by pulsed laser treatment with pulse widths in the nanosecond range and utilised it for adhesive bonding. They described the formation of a highly porous oxide layer and they investigated the chemical modification of the surface. In general, the contaminations on the surface are reduced and the content of oxides is increased. The observed joint strengths of the laser pre-treated specimens were at least equal to those of chemically or electrochemically modified specimens.

3. Experimental setup

3.1. Materials

EN AW 6082 was utilised as metal joining partner. The TP matrices PA 6, PA 66 and PBT with different fibre volume contents and different fibre lengths were chosen. The properties of all materials are listed in Table 4.

Table 4. Properties of the materials.

	Unit	EN AW 6082	PA 6 GF15	PA 66 GF50	PBT GF60 UD
Density	kg/m³	2700	1300	1560	2000
Tensile modulus	GPa	70	6	16,8	33
Tensile strength	MPa	310	95	240	770
Melting temperature	°C		220	260	223
Thickness	mm	2	3	4	2
Fibre length	-		Short fibres	Long fibres	Endless fibres
Fibre mass content	%		15	50	60

3.2. Thermal joining by laser radiation

Thermal joining was performed by HCJ with the aid of a diode laser in the wavelength of 808 nm. The specimens were clamped by a quartz glass and the pressure was applied by a pneumatic pressure cylinder. The dimensions of the specimens are shown in Fig. 2.

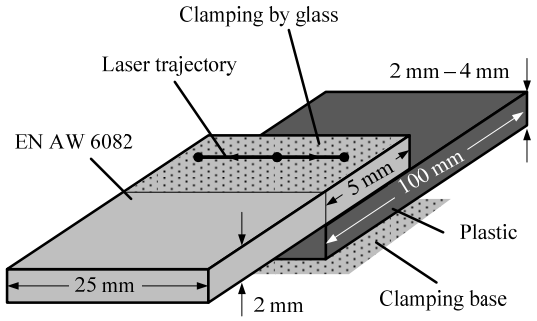

Fig. 2. Dimensions of the specimens and the laser trajectory.

The specimens were arranged and tested with regard to the tensile shear strength based on DIN EN 1465. In order to compare the tensile shear strength of all employed materials, the overlap was incrementally decreased from 12.5 mm until no fracture in the base material of the weakest plastic, PA 6 GF15, was observed. The final overlap of the specimens was set to 5 mm (overlap area A = 125 mm²). To create a uniform temperature distribution, the laser spot was defocused to an estimated spot diameter of 8 mm and the laser beam was stopped for three times on the joining trajectory while radiating onto the metal surface. Further constraints of the joining process are shown in Table 5.

Table 5. Settings for the heat conduction joining experiments with laser radiation.

	Unit	Setting
Laser power	W	250 - 500
Laser spot diameter	mm	8
Joining time	s	10 - 15
Applied pressure	bar	4

4. Results and discussion

4.1 Surface pre-treatment for the metal joining partner

Three different laser structures have been manufactured in the regime of Group II (macroscopic structure), Group III (microscopic structure) and Group IV (nanoscopic structure) on EN AW 6082 in order to evaluate their potential for joining with glass fibre reinforced TPs, see Fig. 3. To benchmark those surface pre-treatments, a mechanical pre-treatment was performed by abrasive blasting with medium sized glass beads as abrasive media and a pressure of 4 bar.

The macroscopic structure was manufactured using Surfi-Sculpt, while the laser trajectory was arranged in a star configuration with 16 arms. By guiding the laser beam from the centre of the star outwards, a feature was built up in the middle of the star, see Fig. 3a. Multiple features were arranged onto the overlap area with a distance of 3 mm in between. In order to create a pin height of 1.2 mm, the laser beam was passed over each arm of the stars for five times. In earlier investigations, the selected pin height has been proven to provide the best mechanical properties for metal TP joints.

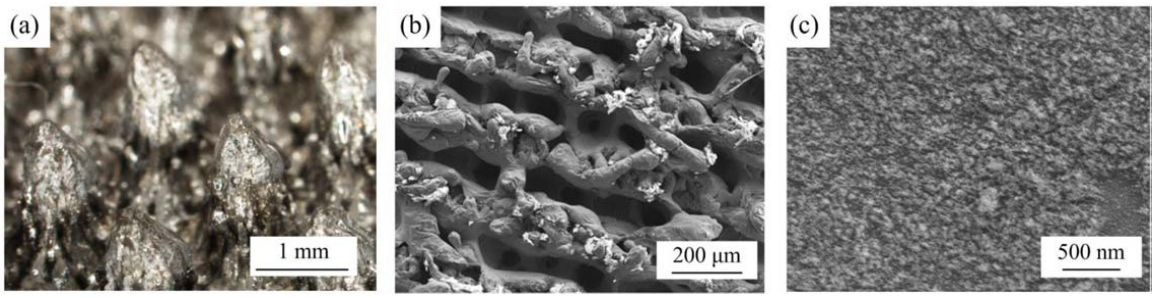

Fig. 3. (a) Macroscopic; (b) microscopic and (c) nanoscopic surface structure.

The microscopic surface structure was generated by employing a cw-laser source and a modified remote ablation cutting (RAC) process. In RAC, the material in the interaction zone is partially evaporated and the remaining melt is ejected by the vapour pressure (Zaeh et al. 2010, Musiol et al. 2011). As a consequence, a kerf is formed. The microscopic pattern was manufactured by a continuous scan movement of the laser spot over the metal with a line distance of 0.2 mm. In order to create a uniform grid structure, the scanning was repeated with an angle of 60° and 120° to the original direction. The SEM picture in Fig. 3b shows the surface having large undercuts. In recent research of Amend et al. (2013), the generated structure depth of approximately 200 µm was found to be a good basis for a high joint strength.

The nanoscopic structure was manufactured according to the publications listed in Table 3 and is pictured in Fig. 3c. An Yb:fibre laser was employed scanning the whole overlap region in one repetition with pulses in the nanosecond-range.

The manufacturing parameters of the different surface structures are given in Table 6. The highest processing rate was achieved by utilising the microscopic structure. The process of nanoscopic structuring was about seven times and the macroscopic structuring was about 140 times slower.

Table 6. Parameters for the manufactured surfaces.

	Unit	Macroscopic structure	Microscopic structure	Nanoscopic structure
Laser power	W	900	1000	20
Scan velocity	mm/s	1000	10000	500
Pulse repetition rate	kHz	-	-	20
Processing rate (estimated)	cm^2/s	0,05	7	1

With regard to an upscale potential of the processes it is expected that the processing rate of the pulsed laser pre-treatment directly correlates with the average laser power. In contrast, the macroscopic and microscopic processes may be restricted either due to the energy input or to the scan velocity.

That the comparably high energy input of the cw-laser radiation already affects these structures is pictured in Fig. 4, in which cracks and cavities are visible.

Aluminium alloys and in particular EN AW 6082 are susceptible to the formation of hot cracks during welding processes. Those occur throughout the cooling of the molten aluminium due to the different solidification temperatures of the individual alloying elements. One element may already be solid, while another is still in the molten state. The resulting additional shrinkage stresses may then cause hot cracking. Hot cracking can be avoided either by modifying the elements in the alloy or changing the processing parameters, for example by pre- and post-heating of the specimens which can be subject to further investigations. (Leimser 2009)

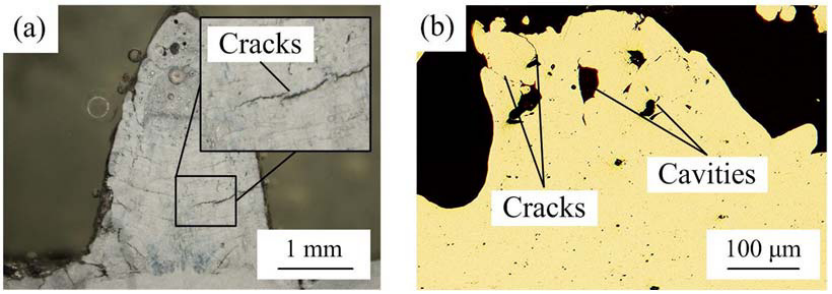

Fig. 4. Cross section of a macroscopic structure (a) and a microscopic structure (b).

4.2 Mechanical strength of the hybrid joints

After laser pre-treating the metal specimens, HCJ was performed and the mechanical strength was evaluated by a lap shear test. The results are given in Fig. 5. Both the short fibre reinforced PA 6 GF15, the long fibre reinforced PA 66 GF50 and the endless fibre reinforced PBT GF60 UD were joined to the different laser structured and abrasive blasted aluminium specimens. For defined surface conditions, all specimens were cleaned with isopropyl alcohol prior to joining. The mean values and the error bars are calculated from at least three repetitions for each surface pre-treatment.

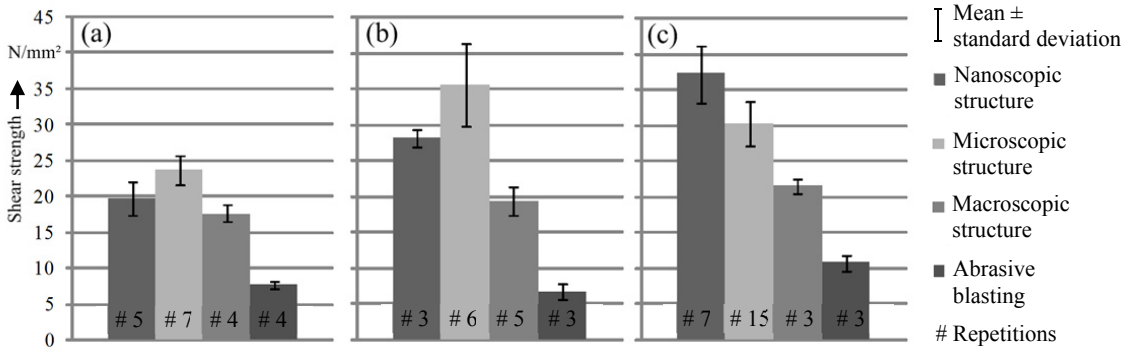

Fig. 5. Tensile shear strength for different surface pre-treatments and (a) PA 6 GF15; (b) PA 66 GF50; (c) PBT GF60 UD.

The processing parameters for HCJ had to be adjusted for each TP due to the different melting temperatures of the materials, see Table 4. Furthermore, it was necessary to regulate the energy input depending on the surface pre-treatment. Since the energy between the specimens is transferred by heat conduction, a large surface area in contact, e.g. for the nanoscopic structure, leads to an increase in conductivity in contrast to a smaller surface area in contact, e.g. for the macroscopic structure.

From the results shown in Fig. 5 it becomes obvious that the mean strength of the PA 6 GF15 joints is lower than for the remaining materials. Since PA 6 GF15 has the weakest mechanical properties (e.g. tensile modulus) compared to PA 66 GF50 and PBT GF60 UD, it may be exposed to the highest peeling stress in the utilised single-shear overlap configuration. This leads to an impact on the shear strength (Habenicht 2009).

The resistance against peeling is dependent on the elastic modulus, the thickness, the overlap length of the adhesive (here TP) as well as the adherent and increases by enlargement of the named properties. In addition, it is reported that the peeling resistance can be influenced by the addition of glass fibres or glass fabrics, since they allow a better transmission of the peeling stress to other regions of the joint. (Habenicht 2009)

Thus, the specimens with PA 66 GF50 and PBT GF60 UD are exposed to less peeling stress and consequently a high shear strength of up to 42 N/mm². Besides good joint qualities, these high values are obtained due to the

overlap length of only 5 mm and a decrease in the joint strength is expected with an increase in the overlap length, which is subject to ongoing investigations.

The abrasive blasting as surface pre-treatment provides the lowest shear strength for all materials ranging from about 6 N/mm² to 11 N/mm² since it has only minor influence on the surface topography and chemical composition of the metal. The fracture plane for PBT GF60 UD shows mainly adhesive failures, see Fig. 6a. Barely residues of the TP matrix can be indicated on the metal surface.

An increased joint strength in comparison to the abrasive blasting was obtained by the macroscopic surface pre-treatment, ranging from 17 N/mm² to 21 N/mm². Fig. 6b shows that the Surfi-Sculpt features were bent or broken while applying load on the specimens. The fracture plane exhibits only adhesive failure for the matrix which implicates that the joint strength mostly depends on the strength of the manufactured features. Again the strength of the Surfi-Sculpt features seems to be limited by hot cracks shown in Fig. 4a.

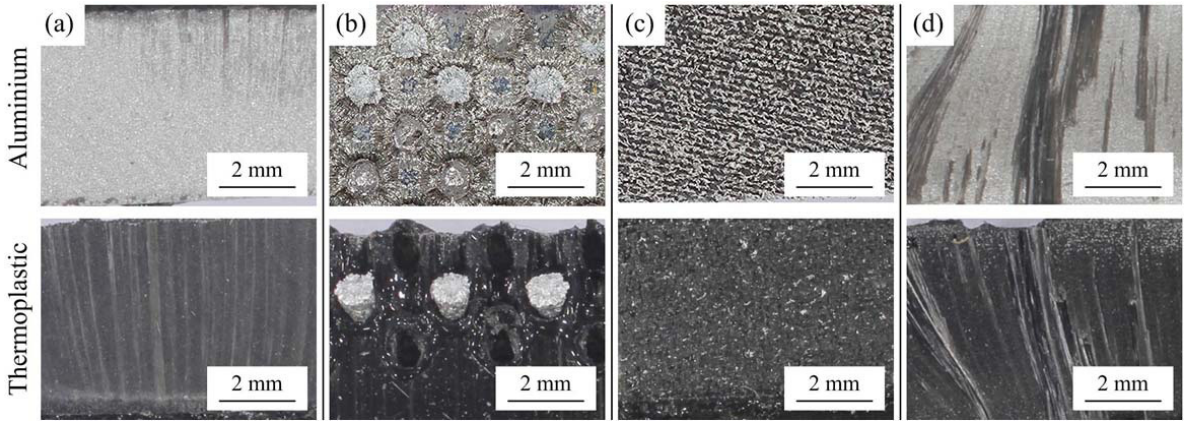

Fig. 6. Fracture planes for PBT GF60 UD and (a) abrasive blasting; (b) macroscopic structure; (c) microscopic structure; (d) nanoscopic structure.

The best joint strength for PA 6 GF15 and PA 66 GF50 was obtained with the microscopic surface structure. In Fig. 7a it can be seen that the TP penetrates well into the microscopic cavities. Only a few air pockets were examined for the short and long fibre reinforced materials. In contrast, only minor TP residues are detected in the cross section when PBT GF60 UD is in use, see Fig. 7b. This indicates that due to the unidirectional alignment and the fibre length less TP material is able to infiltrate the cavities. Consequently, a decrease of the joint strength is observed for the microscopic structure in combination with the endless fibre reinforced TP, see Fig. 5b/c. For all TPs, metal residues of the microscopic structure have been identified at the fracture plane of the matrix as shown in Fig. 6c. This can be explained by the hot cracks and cavities according to Fig. 4b which weaken the structure.

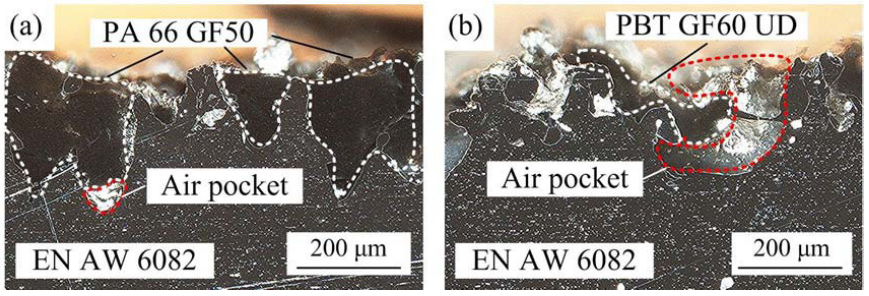

Fig. 7. Cross section of the microscopic structure after tensile test with (a) PA 66 GF50; (b) PBT GF60 UD.

In case of employing the PBT GF60 UD, the best joint strength is achieved by the nanoscopic structure, see Fig. 5c. The fracture plane of the metal, shown in Fig. 6d, is covered by TP and glass fibres which indicate a good force transmission among the joining partners. In addition, no cracks were observed for the nanoscopic structure since the energy input of the manufacturing process is about 50 times less in comparison to the macroscopic and microscopic processes. Yet it was detected that some oxide particles were detached from the metal surface which now adhere to the TP interface, see Fig. 6d. This indicates that an improved adhesion of the oxide layer to the metal substrate could lead to a further increase of the joint strength.

5. Conclusion and outlook

In the presented work, aluminium sheets were pre-treated by laser radiation. Subsequently the specimens were joined to glass fibre reinforced TPs, with different fibre length and fibre content, by laser-based heat conduction joining. According to the state of the art, four categories of structure sizes for the laser surface pre-treatment were identified.

Among these categories are the macroscopic, microscopic and nanoscopic structures which were processed and investigated with regard to mechanical strength and processing rate. The macroscopic structure was manufactured by the use of cw-laser radiation and with the aid of the Surfi-Sculpt process. A modified remote ablation cutting process was employed in order to generate the microscopic structure. In contrast, a pulsed laser system with pulses in the nanosecond range was used to create the nanoscopic structure.

In general, the laser-based heat conduction joining with a glass plate as a clamping device offers a reproducible joining result with shear strengths of up to 42 N/mm², depending on the surface pre-treatment and the allocated material. In order to obtain steady joining results, the energy input had to be adjusted to the TP material and the surface pre-treatment which were in use.

The results of the tensile shear tests showed that for PA 6 GF15 the mean joint strength was lower than for the remaining materials. The reduction in shear strength indicated that higher peel stresses occur which were caused by the low tensile modulus and thickness of the PA 6 GF15 specimens. Further investigations with increased specimen thickness, increased overlap length and equal matrix materials are on the way to address this issue.

For the microscopic structure, the highest processing rate and the best joint strength for the short and long fibre reinforced TPs (PA 6 GF15, PA 66 GF50) was obtained. In contrast, hybrid joints with the nanoscopic structure attained the highest joint strength for the endless fibre reinforced material (PBT GF60 UD). The alteration in tensile strength was explained by the fibre content and the fibre alignment which hinders the endless fibre reinforced TP to infiltrate the microscopic structure.

For all laser surface pre-treatments, metal residues were detected at the fractured TP interface. The residues of the macroscopic and microscopic structures were associated to the hot cracks and the cavities which occur due to the surface pre-treatment process. Because a detachment of the nanoscopic structure was identified as well, it is indicated that an optimisation of all structures with regard to the energy input can lead to a further improvement of the joint strength.

Acknowledgements

The results presented in this paper were gathered within the research project “NexHOS”, funded by the German Federal Ministry for Economic Affairs and Energy (BMWi). The authors thankfully acknowledge its financial support.

References

Abed, S., Knapp, W., 2007. New Applications of Laser Welding in the Field of Thermoplastic Polymer Composites. In: ICALEO 2007 Congress Proceedings, 607–612.

Ageorges, C., Ye, L., 2002. Fusion bonding of polymer composites. Springer. London, New York.

Amend, P., Pfindel, S., Schmidt, M., 2013. Thermal Joining of Thermoplastic Metal Hybrids by Means Of Mono- and Polychromatic Radiation. In: Physics Procedia 41, 98–105.

AVK, 2010. Handbuch Faserverbundkunststoffe. Vieweg + Teubner. Wiesbaden.

Bartl, J.; Baranek, M., 2004. Emissivity of aluminium and its importance for radiometric measurement. In: Measurement Science Review (Volume 4), 31–36.
BASF, 2013. Gelegt, nicht gewoben – BASF mit erstem Tape Demonstratorbauteil auf der K 2013. Philipp, S. Online available at http://www.basf.com/group/pressemitteilungen/P-13-479.
Bergmann, J. P., Stambke, M, 2012. Potential of Laser-manufactured Polymer-metal hybrid Joints. In: Physics Procedia 39, 84–91.
Beyer, E., Ostendorf, A., Poprawe, R, 2013. WLT-White Paper: Tailored Surface. Wissenschaftliche Gesellschaft Lasertechnik e.V. Herbert Utz Verlag GmbH. München.
Blackburn, J., Hilton, P., 2011. Producing Surface Features with a 200 W Yb-fibre Laser and the Surfi-Sculpt® Process. In: Physics Procedia 12, 529–536.
Cenigaonaindia, A., Liébana, F., Lamikiz, A., Echegoyen, Z., 2012. Novel Strategies for Laser Joining of Polyamide and AISI 304. In: Physics Procedia 39, 92–99.
Critchlow, G. W., Cottam, C. A., Brewis, D. M., Emmony, D. C., 1997. Further studies into the effectiveness of CO2-laser treatment of metals for adhesive bonding. In: International Journal of Adhesion and Adhesives 17 (2), 143–150.
Demir, A. G., Maressa, P., Previtali, B., 2013. Fibre Laser Texturing for Surface Functionalization. In: Physics Procedia 41, 759–768.
Earl, C., Hilton, P., O'Neill, B., 2012. Parameter Influence on Surfi-Sculpt Processing Efficiency. In: Physics Procedia 39, 327–335.
Ehrenstein, G. W., 2006. Faserverbund-Kunststoffe. Hanser. München.
Engelmann, C., Roesner, A., Olowinsky, A., Mamuschkin, V., 2013. Lasermikrostrukturen zum lasergestützten Fügen von Kunststoff und Metall. In: DVS Congress 2013, Große Schweißtechnische Tagung, Essen, 179–183.
Flock, D., 2012. Wärmeleitungsfügen hybrider Kunststoff-Metall-Verbindungen. PhD Thesis. Aachen.
Fortunato, A., Cuccolini, G., Ascari, A., Orazi, L., Campana, G., Tani, G., 2010. Hybrid metal-plastic joining by means of laser. In: Int J Mater Form 3 (S1), 1131–1134.
Habenicht, G., 2009. Kleben. Springer. Berlin.
Holtkamp, J., Roesner, A., Gillner, A., 2010. Advances in hybrid laser joining. In: Int J Adv Manuf Technol 47 (9-12), 923–930.
Katayama, S., Kawahito, Y., 2008. Laser direct joining of metal and plastic. In: Scripta Materialia 59 (12), 1247–1250.
Kawahito, Y., Tange, A., Kubota, S., Katayama, S., 2006. Development of Direct Laser Joining for Metal and Plastic. In: ICALEO 2006 Congress Proceeding, 376–382.
Kurtovic, A., Brandl, E., Mertens, T., Maier, H. J., 2013. Laser induced surface nano-structuring of Ti–6Al–4V for adhesive bonding. In: International Journal of Adhesion and Adhesives 45, 112–117.
Leimser, M., 2009. Strömungsinduzierte Einflüsse auf die Nahteigenschaften beim Laserstrahlschweißen von Aluminiumwerkstoffen. PhD Thesis. Stuttgart.
Lu, Y. F., Takai, M., Komuro, S., Shiokawa, T., Aoyagi, Y., 1994. Surface cleaning of metals by pulsed-laser irradiation in air. In: Appl. Phys. A 59 (3), 281–288.
McKinsey & Company, 2012. CO2-Regulierung sorgt bis 2030 für dreistelliges Milliardenwachstum im Leichtbau. Hattrup-Silberberg, M. Online available at http://www.mckinsey.de/co2-regulierung-sorgt-bis-2030-f%C3%BCr-dreistelliges-milliardenwachstum-im-leichtbau.
Mertens, T., Gammel, F. J., Kolb, M., Rohr, O., Kotte, L., Tschöcke, S. et al., 2012. Investigation of surface pre-treatments for the structural bonding of titanium. In: International Journal of Adhesion and Adhesives 34, 46–54.
Musiol, J., Zaeh, M. F., Guertler, M. R., 2011. Contribution on Modelling the Remote Ablation Cutting. In: ICALEO 2011 Congress Proceedings, 369–377.
Niwa, Y., Kawahito, Y., Kubota, S., Katayama S., 2007. Development and Improvement in Laser Direct Joining of Metal and Plastic. In: ICALEO 2007 Congress Proceedings, 463–470.
Rechner, R., 2012. Laseroberflächenvorbehandlung von Aluminium zur Optimierung der Oxidschichteigenschaften für das strukturelle Kleben. PhD Thesis. Dresden.
Rechner, R., Jansen, I., Beyer, E., 2010. Influence on the strength and aging resistance of aluminium joints by laser pre-treatment and surface modification. In: International Journal of Adhesion and Adhesives 30 (7), 595–601.
Roesner, A., Scheik, S., Olowinsky, A., Gillner, A., Reisgen, U., Schleser, M., 2011. Laser Assisted Joining of Plastic Metal Hybrids. In: Physics Procedia 12, 370–377.
Roesner, A., Olowinsky, A., Gillner, A., 2013. Long Term Stability of Laser Joined Plastic Metal Parts. In: Physics Procedia 41, 169–171.
Rotel, M., Zahavi, J., Tamir, S., Buchman, A., Dodiuk, H., 2000. Pre-bonding technology based on excimer laser surface treatment. In: Applied Surface Science 154-155, 610–616.
Turner, M. W., Crouse, P. L., Li, L., Smith, A.J.E., 2006. Investigation into CO2 laser cleaning of titanium alloys for gas-turbine component manufacture. In: Applied Surface Science 252 (13), 4798–4802.
Venables, J. D., 1984. Adhesion and durability of metal-polymer bonds. In: J Mater Sci 19 (8), 2431–2453.
Wahba, M., Kawahito, Y., Katayama, S., 2011. Laser direct joining of AZ91D thixomolded Mg alloy and amorphous polyethylene terephthalate. In: Journal of Materials Processing Technology 211 (6), 1166–1174.
Zaeh, M. F., Moesl, J., Musiol, J., Oefele, F., 2010. Material processing with remote technology revolution or evolution? In: Physics Procedia 5, 19–33.
Zimmermann, S., Specht, U., Spieß, L., Romanus, H., Krischok, S., Himmerlich, M., Ihde, J., 2012. Improved adhesion at titanium surfaces via laser-induced surface oxidation and roughening. In: Materials Science and Engineering: A 558, 755–760.